Continuum Mech. Thermodyn. (2016) 28:1111–1125
DOI 10.1007/s00161-015-0469-7

ORIGINAL ARTICLE

Michael Johlitz · Benedikt Dippel · Alexander Lion

Dissipative heating of elastomers: a new modelling approach based on finite and coupled thermomechanics

Received: 14 April 2015 / Accepted: 17 July 2015 / Published online: 30 July 2015

Abstract Especially in the automotive industries, elastomers take an important role. They are used in different types of bearings, where they inhibit vibration propagation and thereby significantly enhance driving performance and comfort. That is why several models have already been developed to simulate the material's mechanical response to stresses and strains. In many cases, these models are developed under isothermal conditions. Others include the temperature-dependent mechanical behaviour to represent lower stiffness's for higher temperatures. In this contribution it is shown by some exemplary experiments that viscoelastic material heats up under dynamic deformations. Hence, the material's properties change due to the influence of the temperature without changing the surrounding conditions. With some of these experiments, it is shown that a fully coupled material model is necessary to predict the behaviour of bearings under dynamic loads. The focus of this contribution lies on the modelling of the thermoviscoelastic behaviour of elastomers. In a first step, a twofold multiplicative split of the deformation gradient is performed to be able to describe both mechanical and thermal deformations. This concept introduces different configurations. The stress tensors existing on these configurations are used to formulate the stress power in the first law of thermodynamics which allows to simulate the material's self-heating. To formulate the temperature dependency of the mechanical behaviour, the non-equilibrium part of the Helmholtz free energy function is formulated as a function of the temperature and the deformation history. With the introduced model, some FE calculations are carried out to show the model's capability to represent the thermoviscoelastic behaviour including the coupling in both directions.

Keywords Viscoelasticity · Dissipative heating · Thermomechanics · Nonlinear continuum mechanics

1 Introduction and motivation

1.1 State of the art

In a large number of applications, filler-reinforced elastomers play fundamental roles. In the automotive industry, for example, they are used to decouple undesired engine vibrations from car bodies, to generate desired

Communicated by Andreas Öchsner.

M. Johlitz (✉) · B. Dippel · A. Lion
Institute of Mechanics, Universität der Bundeswehr München, Werner-Heisenberg-Weg 39, 85579 Neubiberg, Germany
E-mail: michael.johlitz@unibw.de

B. Dippel
E-mail: benedikt.dippel@unibw.de

A. Lion
E-mail: alexander.lion@unibw.de

elastokinematic properties of vehicle suspensions or to act as material for sealings. In the last application they have to withstand long-term thermal and mechanical loadings or the exposure to chemical substances like oil, benzene or anti-freezing agents. Their relative low costs and low specific weight are additional advantages. In order to utilise these advantages it is necessary to be able to predict and to simulate the behaviour of elastomeric parts under environmental influences, mechanical loads and thermal exposures during their lifetime.

In this context, there are many theoretical and experimental studies from industries, universities and research institutes. Besides their pronounced deformability, filler-reinforced elastomers exhibit a relative large number of inelastic phenomena. At first, the Mullins effect which takes place under large quasi-static deformations and the Payne effect under small dynamic strains should be mentioned (cf. [13,42] or [38] and the citations therein).

The frequency- and rate-dependent material behaviour (cf. [17,40,41] or [20] among many others) or the temperature dependence (cf. [20,24,28] or [50]) is of high importance for applications with oscillating loads. A usual textbook on the elastic and thermoelastic behaviour of elastomers under finite strains has been provided by Treloar [47]. In this book, micro-mechanically based and phenomenological models as well as thermomechanical coupling effects like thermoelastic inversion and the Gough Joule effect are discussed. Based on physical considerations, unfilled elastomers are frequently assumed to behave entropy elastic like an ideal gas such that the stress is a linear function of the thermodynamic temperature. Alts [1] also considered energy elastic contributions to the stress.

In continuum mechanics, there are many articles in which the material behaviour of elastomers is constitutively modelled. To this end, [4,9,21,39] or [35] developed micro-mechanically based models. In [2,11,15,22,27,32,34,36,40,41,44] or [48], phenomenological models of finite nonlinear viscoelasticity or thermoviscoelasticity are proposed. These approaches are formulated using internal variables. The related fundamentals can be found in [8] or [7], and a historical overview over the area of applications is provided by Horstemeyer and Bammann [18].

The multiplicative decomposition of the deformation gradient into several parts with special physical meanings is a frequently applied method. Representative decompositions split the deformation gradient into elastic and viscous or plastic parts, thermal and mechanical parts, volumetric and isochoric parts or combinations of them (cf. [30,33] or [44] and the citations therein). Based on this method, the specific Helmholtz free energy is frequently formulated as the sum of volumetric and isochoric, mechanical and thermal or elastic and inelastic parts. In [31], a hybrid free energy density has been proposed which depends on the pressure, the isochoric part of the deformation, the temperature and internal variables. The advantage of this approach comes to light when the stress strain behaviour of a material in combination with its calorimetric behaviour under isobaric conditions has to be described.

In order to formulate thermodynamically consistent constitutive models, the Clausius–Duhem inequality is taken into account in combination with the expression for the specific free energy of the model (cf. [14]). In many applications, the influence of the temperature on the mechanical material behaviour or of the inelastic energy dissipation of the material to the temperature is irrelevant.

On the other hand, there are also applications in which temperature and dissipation play important factors. In [11,28] experimentally observed temperature changes which are caused by energy dissipation are measured. In suspension bearings or engine mounts of passenger cars, temperature-induced effects have an enormous influence on the mechanical behaviour, the durability properties and the lifetime of the mount. The typical temperature range which is relevant for cars is between $-20\,^{\circ}\mathrm{C}$ in winter up to about $100\,^{\circ}\mathrm{C}$ in the direct vicinity of the engine or during dynamic deformations with large frequencies and amplitudes. Fundamental aspects with regard to dissipation inequalities are discussed in [25,26]. The temperature-dependent elastic or inelastic behaviour of polymers is modelled in [3,5,6,11,29,39] or [43]. Nevertheless, there are many open questions to be answered in the future.

The current article is structured as follows. In the next Sect. 1.2, experimental investigations with regard to the temperature dependence of the stress relaxation and dissipative heating during cyclic loadings are shown. They are used in order to motivate the development of an adequate model. Section 2 is addressed to the derivation of a thermodynamical consistent constitutive model which allows the representation of the thermoviscoelastic behaviour of filler-reinforced elastomers, i.e. which is able to represent the dissipative self-heating of elastomers. In Sect. 3, the model is implemented as a coupled thermomechanical problem into an in-house code. Some exemplary simulations are carried out by solving boundary value problems for a simple geometry. The results are presented and discussed. The paper closes with an outlook to future work.

1.2 Experimental motivation

Since this article is addressed to the development of a consistent framework to represent thermoviscoelastic material properties of filler-reinforced elastomers, only a small number of experiments with regard to temperature dependence and dissipative heating are presented. They are only used to highlight the well-known effects and to motivate the structure of the model which is developed in this paper. For further studies and more detailed investigations the reader is referred to the works of [20,23,28] or [11] and the citations therein.

The investigated elastomer is used in the automotive industry for suspension bearings. It is a carbon black-filled natural rubber compound with a Shore A hardness of 60 and a carbon black content of 50 phr. Its glass transition temperature θ_G is approximately 240 K. In order to analyse the temperature dependence of the material behaviour, relaxation tests under a constant and rapidly applied shear deformation of 5° are driven. In order to eliminate the influence of thermal expansion effects, shear tests were made. The experiments were carried out under isothermal conditions at temperature values of -10, 20, 50 and 80 °C which are far above the glass transition temperature of the elastomer and the holding times were 1200 s. The experimentally observed stress responses which are plotted in Fig. 1 demonstrate that the relaxation is more pronounced when the temperature increases. In order to interpret this effect in terms of thermoviscoelasticity, it can be assumed that the equilibrium stress is entropy elastic such that it depends linearly on the absolute temperature. In addition, it can be assumed that the stress relaxation at the highest temperature of 80 °C is nearly finished after about 1200 s such that the stress has reached its equilibrium value. These assumptions lead to the consequence that the equilibrium stress at -10 °C is only $(273.15 - 10\,\mathrm{K})/(273.15 + 80\,\mathrm{K}) \approx 0.75$ of that at 80 °C leading to a value of about 0.09 MPa. This estimation shows that the temperature dependence of the stress relaxation can be attributed to the overstress. Ignoring the temperature dependence would lead to an oversimplification.

Another important question is concerned to the source of the specimens temperature. Under equilibrium conditions, the most significant influence is the temperature of the environment or the surrounding medium, for example hot air or a cooling fluid. If the external temperature does not change and the mechanical loading processes are quasi-static, the conditions of the specimen remain isothermal. If the loading processes are sufficient fast or the boundary conditions are adiabatic and the elastomer is entropy elastic and shows thermal expansion, the thermoelastic Gough Joule effect can be seen (cf. [47]). In this case, the specimen temperature is a unique function of the deformation. If the elastomer is filler-reinforced, it exhibits also viscoelastic dissipation effects which lead to a pronounced self-heating under dynamic excitations with sufficient high amplitudes and frequencies. In general, all effects are superimposed. In Fig. 2, the changes in the stationary value of the surface temperature of standard tension specimens with a cross-sectional area of 4 mm × 2 mm are plotted as a function of the excitation frequency. With an infra-red camera, the surface temperature is measured and evaluated after constant values were reached. The strain amplitude varies between 5 and 20 % and the static pre-deformation was 30 %. It can be seen that the temperature increases are not negligible and become more pronounced when the amplitude and the frequency increase.

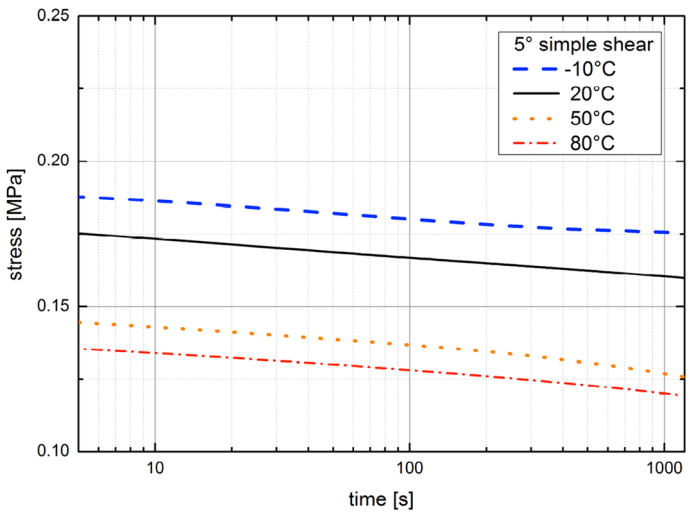

Fig. 1 Simple shear relaxation tests under different temperatures; the higher the temperature, the lower the stress in relaxation tests under 5° of shear

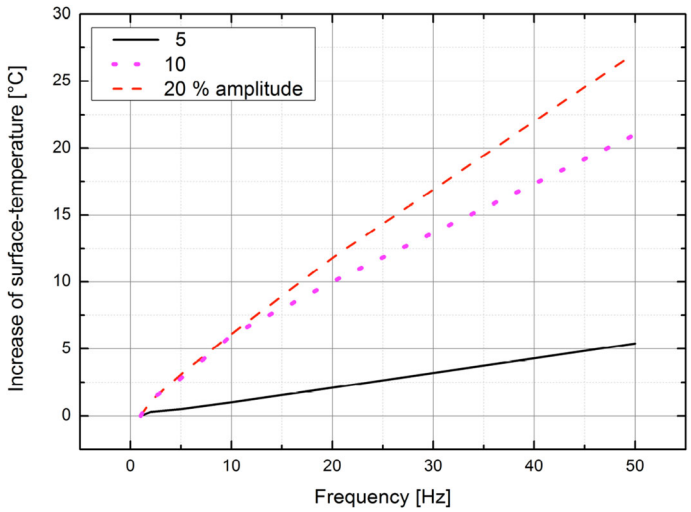

Fig. 2 Self-heating under dynamic tension deformations with different frequencies and amplitudes of 5, 10 and 20 %; measured surface-temperatures are related to the starting temperature of 23 °C

Considering these observations, it is obvious that a bi-directionally coupled thermomechanical formulation of a material model is required, i.e. that dynamical loads induce a significant self-heating of the material (increase in the temperature) and the increase in the temperature again influences the mechanical behaviour in terms of the viscoelasticity (modification of the relaxation behaviour).

2 Modelling

The model is to be used for viscoelastic materials that are subject to large deformations and warm up as a result of alternating stresses due to the dissipated energy. Accordingly, the model is coupled in this way that the dissipated energy converts into heat and therefore affects the heat conduction equation which follows from the first law of thermodynamics.

2.1 Kinematics

From the kinematical point of view, a twofold multiplicative split of the deformation gradient $\mathbf{F}$ is performed in order to describe the thermo-viscoelastic material behaviour. On the one hand, there is a division into a volumetric part $\bar{\mathbf{F}}$ and an isochoric part $\hat{\mathbf{F}}$. On the other hand, the isochoric deformation gradient $\hat{\mathbf{F}}$ is split into an isochoric elastic $\hat{\mathbf{F}}_\mathrm{e}$ and an isochoric inelastic component $\hat{\mathbf{F}}_\mathrm{i}$.

$$\begin{aligned} \mathbf{F} &= \hat{\mathbf{F}} \cdot \bar{\mathbf{F}} \\ \hat{\mathbf{F}} &= \hat{\mathbf{F}}_\mathrm{e} \cdot \hat{\mathbf{F}}_\mathrm{i} \\ \mathbf{F} &= \hat{\mathbf{F}}_\mathrm{e} \cdot \hat{\mathbf{F}}_\mathrm{i} \cdot \bar{\mathbf{F}} \end{aligned} \tag{1}$$

To this end, the volumetric part of $\mathbf{F}$ is defined as

$$\bar{\mathbf{F}} = J^{\frac{1}{3}}\,\mathbf{I} \tag{2}$$

and the isochoric part as

$$\hat{\mathbf{F}} = J^{-\frac{1}{3}}\,\mathbf{F}. \tag{3}$$

$\varepsilon_\mathrm{v} = J - 1 = \det \mathbf{F} - 1$ describes the volumetric strain, wherein $\det \hat{\mathbf{F}} = 1$ is valid for the isochoric part. The kinematics are sketched in Fig. 3. The strain measures of the reference configuration RC are introduced by the

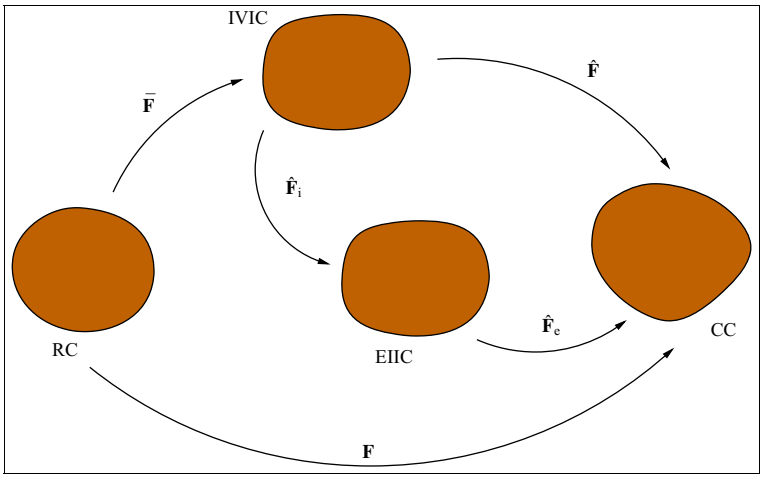

Fig. 3 Multiplicative split and introduction of intermediate configurations

right Cauchy–Green deformation tensor $\mathbf{C}$ and the Green–Lagrange strain tensor $\mathbf{E}$.

$$\begin{aligned} \mathbf{C} &= \mathbf{F}^T \cdot \mathbf{F} \\ \mathbf{E} &= \frac{1}{2}\left(\mathbf{C} - \mathbf{I}\right) \end{aligned} \tag{4}$$

On the current configuration CC, the related quantities are the left Cauchy–Green deformation tensor $\mathbf{B}$ and the Euler–Almansi strain tensor $\mathbf{A}$.

$$\begin{aligned} \mathbf{B} &= \mathbf{F} \cdot \mathbf{F}^T \\ \mathbf{A} &= \frac{1}{2}\left(\mathbf{I} - \mathbf{B}^{-1}\right) \end{aligned} \tag{5}$$

Between the two configurations, the tensors $\mathbf{E}$ and $\mathbf{A}$ can be converted into each other by the push forward and pull back operations, cf. [14].

$$\begin{aligned} \mathbf{A} &= \mathbf{F}^{-T} \cdot \mathbf{E} \cdot \mathbf{F}^{-1} \\ \mathbf{E} &= \mathbf{F}^T \cdot \mathbf{A} \cdot \mathbf{F} \end{aligned} \tag{6}$$

The multiplicative split of the deformation gradient implies the introduction of so-called fictitious intermediate configurations. The volumetric–isochoric split motivates the isochoric–volumetric intermediate configuration IVIC, the elastic–inelastic split of the isochoric deformation gradient a further, elastic–inelastic intermediate configuration EIIC. In order to illustrate this concept, Fig. 3 can be used.

On the isochoric–volumetric intermediate configuration IVIC, a strain tensor $\boldsymbol{\Gamma}_{\mathrm{IV}}$ is established by the volumetric push forward of the Green–Lagrange strain tensor $\mathbf{E}$

$$\begin{aligned} \boldsymbol{\Gamma}_{\mathrm{IV}} &= \bar{\mathbf{F}}^{-T} \cdot \mathbf{E} \cdot \bar{\mathbf{F}}^{-1} = \bar{\mathbf{F}}^{-T} \cdot \frac{1}{2}\left(\mathbf{F}^T \cdot \mathbf{F} - \mathbf{I}\right) \bar{\mathbf{F}}^{-1} \\ &= \frac{1}{2} J^{-\frac{2}{3}} \left(\mathbf{C} - \mathbf{I}\right) = \frac{1}{2}\left(\hat{\mathbf{C}} - \mathbf{I}\right) + \frac{1}{2}\left(\mathbf{I} - \bar{\mathbf{B}}^{-1}\right) \\ &= \hat{\boldsymbol{\Gamma}}_{\mathrm{IV}} + \bar{\boldsymbol{\Gamma}}_{\mathrm{IV}}. \end{aligned} \tag{7}$$

Thus, the resulting strain tensor on the IVIC can be additively decomposed into the sum of an isochoric part $\hat{\boldsymbol{\Gamma}}_{\mathrm{IV}}$ and a volumetric part $\bar{\boldsymbol{\Gamma}}_{\mathrm{IV}}$. In comparison with other theories (cf. [14,19]), no thermal–mechanical split of the deformation gradient is introduced. Rather, in this approach the properties of the thermal volume expansion are integrated in the volumetric part of the deformation gradient. The big advantage of this approach can be seen while deriving the stress power and the free energy function. It allows for a separately identification of caloric and mechanical material properties. Furthermore, the evolution equations which will be introduced

in order to model the viscoelastic behaviour, have a deviatoric form, cf. [44]. The following mathematical relationships are still valid:

$$\begin{aligned}\bar{\mathbf{C}} &= \bar{\mathbf{F}}^T \cdot \bar{\mathbf{F}} = J^{\frac{2}{3}}\,\mathbf{I}\\ \hat{\mathbf{C}} &= \hat{\mathbf{F}}^T \cdot \hat{\mathbf{F}} = J^{-\frac{2}{3}}\,\mathbf{C}\\ \bar{\mathbf{B}} &= \bar{\mathbf{F}} \cdot \bar{\mathbf{F}}^T = J^{\frac{2}{3}}\,\mathbf{I}\end{aligned} \tag{8}$$

as well as

$$\det \hat{\mathbf{C}} = 1 \Rightarrow \left(\det \hat{\mathbf{C}}\right)^{\cdot} = \frac{\partial \det \hat{\mathbf{C}}}{\partial \hat{\mathbf{C}}} : \dot{\hat{\mathbf{C}}} = \hat{\mathbf{C}}^{-1} : \dot{\hat{\mathbf{C}}} = 0. \tag{9}$$

Consequently, the two tensors $\hat{\mathbf{C}}^{-1}$ and $\dot{\hat{\mathbf{C}}}$ are orthogonal to each other. Based on this fictitious isochoric–volumetric intermediate configuration, one additional configuration is now introduced. The so-called isochoric elastic–inelastic intermediate configuration EIIC is also depicted in Fig. 3. We start with the multiplicative split of the isochoric deformation gradient $\hat{\mathbf{F}}$ into an isochoric elastic component $\hat{\mathbf{F}}_\mathrm{e}$ and an isochoric inelastic one $\hat{\mathbf{F}}_\mathrm{i}$,

$$\hat{\mathbf{F}} = \hat{\mathbf{F}}_\mathrm{e} \cdot \hat{\mathbf{F}}_\mathrm{i}. \tag{10}$$

The motivation for this purpose provides a connection of a spring and a damper in series. This so-called Maxwell element is able to describe viscoelastic material behaviour in the form of a non-equilibrium stress which is also denoted as overstress. The operating strain tensor $\hat{\mathbf{\Gamma}}_\mathrm{EI}$ on the EIIC is obtained by the push forward of the isochoric strain tensor $\hat{\mathbf{\Gamma}}_\mathrm{IV}$ by use of the arithmetic operation

$$\begin{aligned}\hat{\mathbf{\Gamma}}_\mathrm{EI} &= \hat{\mathbf{F}}_\mathrm{i}^{-T} \cdot \hat{\mathbf{\Gamma}}_\mathrm{IV} \cdot \hat{\mathbf{F}}_\mathrm{i}^{-1} = \hat{\mathbf{F}}_\mathrm{i}^{-T} \cdot \frac{1}{2}\left(\hat{\mathbf{F}}^T \cdot \hat{\mathbf{F}} - \mathbf{I}\right) \cdot \hat{\mathbf{F}}_\mathrm{i}^{-1}\\ &= \frac{1}{2}\left(\hat{\mathbf{F}}_\mathrm{e}^T \cdot \hat{\mathbf{F}}_\mathrm{e} - \hat{\mathbf{F}}_\mathrm{i}^{-T} \cdot \hat{\mathbf{F}}_\mathrm{i}^{-1}\right) = \frac{1}{2}\left(\hat{\mathbf{C}}_\mathrm{e} - \mathbf{I}\right) + \frac{1}{2}\left(\mathbf{I} - \hat{\mathbf{B}}_\mathrm{i}^{-1}\right)\\ &= \hat{\mathbf{\Gamma}}_\mathrm{e} + \hat{\mathbf{\Gamma}}_\mathrm{i}\end{aligned} \tag{11}$$

with the right isochoric elastic deformation tensor $\hat{\mathbf{C}}_\mathrm{e} = \hat{\mathbf{F}}_\mathrm{e}^T \cdot \hat{\mathbf{F}}_\mathrm{e}$ and the left isochoric inelastic deformation tensor $\hat{\mathbf{B}}_\mathrm{i} = \hat{\mathbf{F}}_\mathrm{i} \cdot \hat{\mathbf{F}}_\mathrm{i}^T$. This approach ensures again the additive split of the associated deformation measures on this configuration. Physically, the first component describes the deformation of the spring and the second component represents the deformation of the damper of the Maxwell element.

Here, from considerations of the volume conservation of isochoric deformation tensors, another mathematical condition can be derived, too. Starting from the isochoric inelastic deformation gradient $\hat{\mathbf{F}}_\mathrm{i}$ yields

$$\det \hat{\mathbf{F}}_\mathrm{i} = 1 \Rightarrow \left(\det \hat{\mathbf{F}}_\mathrm{i}\right)^{\cdot} = \hat{\mathbf{F}}_\mathrm{i}^{-T} : \dot{\hat{\mathbf{F}}}_\mathrm{i} = \mathrm{tr}\left(\dot{\hat{\mathbf{F}}}_\mathrm{i} : \hat{\mathbf{F}}_\mathrm{i}^{-T}\right) = \mathrm{tr}\left(\hat{\mathbf{L}}_\mathrm{i}\right) = 0 \tag{12}$$

with the spatial isochoric inelastic velocity gradient $\hat{\mathbf{L}}_\mathrm{i}$. The consequence that the trace of $\hat{\mathbf{L}}_\mathrm{i}$ is equal to zero ensures later for a deviatoric shape of the corresponding evolution equation. With this definition, the spatial isochoric inelastic deformation velocity tensor follows to

$$\hat{\mathbf{D}}_\mathrm{i} = \frac{1}{2}\left(\hat{\mathbf{L}}_\mathrm{i} + \hat{\mathbf{L}}_\mathrm{i}^T\right) \Rightarrow \mathrm{tr}\,\hat{\mathbf{D}}_\mathrm{i} = 0. \tag{13}$$

2.2 Stress tensors

This subsection will now represent the required stress tensors and their interrelationships. The second Piola–Kirchhoff stress tensor $\mathbf{S}$ operates on the RC. It can be calculated by the pull back of the Cauchy stress tensor $\mathbf{T}$ by using the relation

$$\mathbf{S} = J\,\mathbf{F}^{-1} \cdot \mathbf{T} \cdot \mathbf{F}^{-T}. \tag{14}$$

The Cauchy stress tensor in volumetric–deviatoric representation reads

$$\mathbf{T} = -p\,\mathbf{I} + \mathbf{T}^{\mathrm{D}}. \tag{15}$$

From modelling hyperelastic materials, it is known that p acts as an undetermined Lagrange multiplier which corresponds to the constitutively undetermined hydrostatic pressure in the case of incompressibility. In this contribution the parameter p is a function of the volumetric expansion J and the temperature θ. Hence, a constitutive equation will be derived while evaluating the second law of thermodynamics. In order to map nearly mechanically incompressible material behaviour, the mechanical part of p together with the bulk modulus K can be numerically used as a penalty factor. The relationship between the Cauchy stresses and the second Piola–Kirchhoff stresses can be obtained by using the concept of dual variables, see [16]. In analogy to this concept, also the stress tensor $\mathbf{T}_{\mathrm{IV}}$ can be introduced. This stress tensor is operating on the IVIC and can be described via

$$\mathbf{T}_{\mathrm{IV}} = \hat{J}\,\hat{\mathbf{F}}^{-1} \cdot \mathbf{T} \cdot \hat{\mathbf{F}}^{-T} \tag{16}$$

with $\hat{J} = \det \hat{\mathbf{F}} = 1$. Based on these considerations, a new stress tensor is now defined on the IVIC, which results from the pull back of the deviator of the Cauchy stress tensor,

$$\hat{\mathbf{T}} = \hat{J}\,\hat{\mathbf{F}}^{-1} \cdot \mathbf{T}^{\mathrm{D}} \cdot \hat{\mathbf{F}}^{-T}. \tag{17}$$

Taking into account the isochoric–volumetric decomposition of the deformation gradient $\mathbf{F}$, the second Piola–Kirchhoff stress tensor can be formulated as follows:

$$\mathbf{S} = -p\,J^{\frac{1}{3}}\hat{\mathbf{C}}^{-1} + J^{\frac{1}{3}}\,\hat{\mathbf{T}}. \tag{18}$$

Thus, the stress power $\mathbf{S} : \dot{\mathbf{E}}$ in terms of quantities operating on the reference configuration is calculated. After a few steps of calculation and rearranging the terms, the following intermediate result appears:

$$\begin{aligned} \mathbf{S} : \dot{\mathbf{E}} = &-\frac{p\,\dot{J}}{3}\hat{\mathbf{C}}^{-1} : \left(\mathbf{I} + 2\,\hat{\boldsymbol{\Gamma}}_{\mathrm{IV}}\right) - p\,J\,\hat{\mathbf{C}}^{-1} : \dot{\hat{\boldsymbol{\Gamma}}}_{\mathrm{IV}} \\ &+ J\,\hat{\mathbf{T}} : \dot{\hat{\boldsymbol{\Gamma}}}_{\mathrm{IV}} + \frac{\dot{J}}{3}\,\hat{\mathbf{T}} : \left(\mathbf{I} + 2\,\hat{\boldsymbol{\Gamma}}_{\mathrm{IV}}\right). \end{aligned} \tag{19}$$

By utilising the relationships

$$\begin{aligned} \hat{\mathbf{C}}^{-1} : \left(\mathbf{I} + 2\,\hat{\boldsymbol{\Gamma}}_{\mathrm{IV}}\right) &= \hat{\mathbf{C}}^{-1} : \hat{\mathbf{C}} = \operatorname{tr}\left(\hat{\mathbf{C}}^{-1} : \hat{\mathbf{C}}\right) = 3 \\ \hat{\mathbf{C}}^{-1} : \dot{\hat{\boldsymbol{\Gamma}}}_{\mathrm{IV}} &= \frac{1}{2}\hat{\mathbf{C}}^{-1} : \dot{\hat{\mathbf{C}}} = 0 \\ \hat{\mathbf{T}} : \left(\mathbf{I} + 2\,\hat{\boldsymbol{\Gamma}}_{\mathrm{IV}}\right) &= \hat{J}\,\hat{\mathbf{F}}^{-1} \cdot \mathbf{T}^{\mathrm{D}} \cdot \hat{\mathbf{F}}^{-T} : \hat{\mathbf{C}} = \operatorname{tr} \mathbf{T}^{\mathrm{D}} = 0, \end{aligned} \tag{20}$$

the stress power can be simplified to

$$\mathbf{S} : \dot{\mathbf{E}} = -p\,\dot{J} + J\,\hat{\mathbf{T}} : \dot{\hat{\boldsymbol{\Gamma}}}_{\mathrm{IV}}. \tag{21}$$

This expression plays an important role in the next section when formulating the material model and was the first time used in the work of [31].

2.3 Material model

The material model, which is developed in this subsection, is designed to represent the thermo-viscoelastic behaviour of elastomers. The starting point is the Clausius–Duhem inequality in terms of the reference configuration

$$-\rho_0\,\dot{\psi}+\mathbf{S}:\dot{\mathbf{E}}-\rho_0\,s\,\dot{\theta}-\frac{\mathbf{Q}}{\theta}\cdot\operatorname{Grad}\theta\geq 0 \tag{22}$$

with the specific Helmholtz free energy ψ, the specific entropy s, the absolute temperature θ, the heat flux vector $\mathbf{Q}$ and the density ρ_0. Concerning thermo-viscoelastic material behaviour, the approach of the Helmholtz free energy function ψ is formulated by using the process variables $J,\theta,\hat{\mathbf{C}},\hat{\mathbf{C}}_\mathrm{e}$. In this case, there is made use of a constitutive assumption which allows for an additive split of the free energy function.

$$\psi=\psi_\mathrm{eq}^\mathrm{vol}(J,\theta)+\psi_\mathrm{eq}^\mathrm{iso}(\hat{\mathbf{C}})+\psi_\mathrm{neq}(\hat{\mathbf{C}}_\mathrm{e}) \tag{23}$$

This assumption implies that the equilibrium behaviour of the material under isochoric processes is temperature independent. Thus, entropy elasticity is not taken into account in this approach. Consequently, the time derivative results to

$$\begin{aligned}\dot{\psi}=&\frac{\partial\psi_\mathrm{eq}^\mathrm{vol}(J,\theta)}{\partial J}\dot{J}+\frac{\partial\psi_\mathrm{eq}^\mathrm{vol}(J,\theta)}{\partial\theta}\dot{\theta}\\&+\frac{\partial\psi_\mathrm{eq}^\mathrm{iso}(\hat{\mathbf{C}})}{\partial\hat{\mathbf{C}}}:\dot{\hat{\mathbf{C}}}+\frac{\partial\psi_\mathrm{neq}(\hat{\mathbf{C}}_\mathrm{e})}{\partial\hat{\mathbf{C}}_\mathrm{e}}:\dot{\hat{\mathbf{C}}}_\mathrm{e}.\end{aligned} \tag{24}$$

Taking into account the split of the stress power from Sect. 2.2, Eq. (21) in combination with the following relationships

$$\begin{aligned}\dot{\hat{\boldsymbol{\Gamma}}}_\mathrm{IV}&=\frac{1}{2}\dot{\hat{\mathbf{C}}}\\\dot{\hat{\mathbf{C}}}_\mathrm{e}&=\hat{\mathbf{F}}_\mathrm{i}^{-T}\cdot\dot{\hat{\mathbf{C}}}\cdot\hat{\mathbf{F}}_\mathrm{i}^{-1}-\hat{\mathbf{L}}_\mathrm{i}^{T}\cdot\hat{\mathbf{C}}_\mathrm{e}-\hat{\mathbf{C}}_\mathrm{e}\cdot\hat{\mathbf{L}}_\mathrm{i}\\\frac{\partial\psi_\mathrm{neq}}{\partial\hat{\mathbf{C}}_\mathrm{e}}:\dot{\hat{\mathbf{C}}}_\mathrm{e}&=\frac{\partial\psi_\mathrm{neq}}{\partial\hat{\mathbf{C}}_\mathrm{e}}:\left(\hat{\mathbf{F}}_\mathrm{i}^{-T}\cdot\dot{\hat{\mathbf{C}}}\cdot\hat{\mathbf{F}}_\mathrm{i}^{-1}\right)-\frac{\partial\psi_\mathrm{neq}}{\partial\hat{\mathbf{C}}_\mathrm{e}}:\left(\hat{\mathbf{C}}_\mathrm{e}\cdot\hat{\mathbf{L}}_\mathrm{i}+\hat{\mathbf{L}}_\mathrm{i}^{T}\cdot\hat{\mathbf{C}}_\mathrm{e}\right)\end{aligned} \tag{25}$$

the second law of thermodynamics can be rewritten as follows:

$$\begin{aligned}&-\left(p+\rho_0\frac{\partial\psi_\mathrm{eq}^\mathrm{vol}}{\partial J}\right)\dot{J}-\left(\rho_0\,s+\rho_0\frac{\partial\psi_\mathrm{eq}^\mathrm{vol}}{\partial\theta}\right)\dot{\theta}-\frac{\mathbf{Q}}{\theta}\cdot\operatorname{Grad}\theta\\&+\left(\frac{1}{2}\,J\,\hat{\mathbf{T}}-\rho_0\frac{\partial\psi_\mathrm{eq}^\mathrm{iso}}{\partial\hat{\mathbf{C}}}-\rho_0\,\hat{\mathbf{F}}_\mathrm{i}^{-1}\cdot\frac{\partial\psi_\mathrm{neq}}{\partial\hat{\mathbf{C}}_\mathrm{e}}\cdot\hat{\mathbf{F}}_\mathrm{i}^{-T}\right):\dot{\hat{\mathbf{C}}}\\&+\rho_0\frac{\partial\psi_\mathrm{neq}}{\partial\hat{\mathbf{C}}_\mathrm{e}}:\left(\hat{\mathbf{C}}_\mathrm{e}\cdot\hat{\mathbf{L}}_\mathrm{i}+\hat{\mathbf{L}}_\mathrm{i}\cdot\hat{\mathbf{C}}_\mathrm{e}\right)\geq 0\end{aligned} \tag{26}$$

The evaluation of this inequality is based on the argumentation of [8] and additionally by taking into account the isochoric structure of $\dot{\hat{\mathbf{C}}}$. It results in the following constitutive relationships

$$\begin{aligned}p&=-\rho_0\frac{\partial\psi_\mathrm{eq}^\mathrm{vol}}{\partial J}\\\rho_0\,s&=-\rho_0\frac{\partial\psi_\mathrm{eq}^\mathrm{vol}}{\partial\theta}\\\mathbf{Q}&=-\lambda_\theta\operatorname{Grad}\theta\\J\,\hat{\mathbf{T}}&=2\,\rho_0\frac{\partial\psi_\mathrm{eq}^\mathrm{iso}}{\partial\hat{\mathbf{C}}}+2\,\rho_0\,\hat{\mathbf{F}}_\mathrm{i}^{-1}\cdot\frac{\partial\psi_\mathrm{neq}}{\partial\hat{\mathbf{C}}_\mathrm{e}}\cdot\hat{\mathbf{F}}_\mathrm{i}^{-T}+\Phi\,\hat{\mathbf{C}}^{-1}\end{aligned} \tag{27}$$

with the coefficient of thermal conductivity λ_θ in Fourier's law of heat conduction. Since only five components of the tensor $\dot{\hat{\mathbf{C}}}$ can be selected freely, its sixth component follows from the incompressibility constraint. Therefore, by evaluating Eq. $(27)_4$ and taking into account Eq. (9), the term $\Phi\,\hat{\mathbf{C}}^{-1}$ is introduced. The function

ϕ must be determined in this way that the stress tensor $\hat{\mathbf{T}}$ has a deviatoric form after transportation to the CC. By calculation of

$$\mathbf{T}^{\mathrm{D}} = \hat{\mathbf{F}} \cdot \hat{\mathbf{T}} \cdot \hat{\mathbf{F}}^{T} \tag{28}$$

and calculating the expression tr $\mathbf{T}^{\mathrm{D}} = \mathbf{I} : \mathbf{T}^{\mathrm{D}} = 0$ the function Φ can be determined to

$$\Phi = -\frac{2}{3}\left(\frac{\partial \psi_{\mathrm{eq}}^{\mathrm{iso}}}{\partial \hat{\mathbf{C}}} : \hat{\mathbf{C}} + \frac{\partial \psi_{\mathrm{neq}}}{\partial \hat{\mathbf{C}}_{\mathrm{e}}} : \hat{\mathbf{C}}_{\mathrm{e}}\right) \tag{29}$$

It now still remains to evaluate the dissipation inequality. Assuming that ψ_{neq} is an isotropic tensor function and the tensor $\hat{\mathbf{C}}_{\mathrm{e}}$ is symmetric, the rule

$$\hat{\mathbf{C}}_{\mathrm{e}} \cdot \frac{\partial \psi_{\mathrm{neq}}}{\partial \hat{\mathbf{C}}_{\mathrm{e}}} = \frac{\partial \psi_{\mathrm{neq}}}{\partial \hat{\mathbf{C}}_{\mathrm{e}}} \cdot \hat{\mathbf{C}}_{\mathrm{e}} \tag{30}$$

applies and therefore, the inequality yields

$$\rho_0 \frac{\partial \psi_{\mathrm{neq}}}{\partial \hat{\mathbf{C}}_{\mathrm{e}}} : \left(\hat{\mathbf{C}}_{\mathrm{e}} \cdot \hat{\mathbf{L}}_{\mathrm{i}} + \hat{\mathbf{L}}_{\mathrm{i}} \cdot \hat{\mathbf{C}}_{\mathrm{e}}\right) = 2\,\rho_0\,\hat{\mathbf{C}}_{\mathrm{e}} \cdot \frac{\partial \psi_{\mathrm{neq}}}{\partial \hat{\mathbf{C}}_{\mathrm{e}}} : \hat{\mathbf{D}}_{\mathrm{i}} \geq 0 \tag{31}$$

with

$$\hat{\mathbf{D}}_{\mathrm{i}} = \frac{1}{2}\left(\hat{\mathbf{L}}_{\mathrm{i}} + \hat{\mathbf{L}}_{\mathrm{i}}^{T}\right). \tag{32}$$

Thus, an evolution equation for the tensor $\hat{\mathbf{D}}_{\mathrm{i}}$ is derived by introducing a proportionality function $\eta(\theta)$. $\eta(\theta) \geq 0$ has the physical meaning of a temperature-dependent viscosity function. It follows

$$\hat{\mathbf{D}}_{\mathrm{i}} = \frac{1}{\eta(\theta)} 2\,\rho_0\,\hat{\mathbf{C}}_{\mathrm{e}} \cdot \frac{\partial \psi_{\mathrm{neq}}}{\partial \hat{\mathbf{C}}_{\mathrm{e}}} + \beta\,\mathbf{I}. \tag{33}$$

Again, the function β has to be determined such that the constraint tr $\hat{\mathbf{D}}_{\mathrm{i}} = 0$ is satisfied, i.e. $\hat{\mathbf{D}}_{\mathrm{i}}$ must have a deviatoric form. Through the calculation of tr $\hat{\mathbf{D}}_{\mathrm{i}} = 0$ the expression

$$\beta = -\frac{2\,\rho_0}{3\,\eta(\theta)} \frac{\partial \psi_{\mathrm{neq}}}{\partial \hat{\mathbf{C}}_{\mathrm{e}}} : \hat{\mathbf{C}}_{\mathrm{e}} \tag{34}$$

is obtained and finally leads to

$$\hat{\mathbf{D}}_{\mathrm{i}} = \frac{2\,\rho_0}{\eta(\theta)}\left(\hat{\mathbf{C}}_{\mathrm{e}} \cdot \frac{\partial \psi_{\mathrm{neq}}}{\partial \hat{\mathbf{C}}_{\mathrm{e}}} - \frac{1}{3}\left(\frac{\partial \psi_{\mathrm{neq}}}{\partial \hat{\mathbf{C}}_{\mathrm{e}}} : \hat{\mathbf{C}}_{\mathrm{e}}\right)\mathbf{I}\right). \tag{35}$$

Hence, a set of general constitutive equations and evolution equations for the description of thermo-viscoelastic elastomers is available.

2.4 Derivation of the equations for the Neo-Hookean model

The next point is the specification of the material functions. To this end, the well-known Neo-Hookean model is applied, cf. [37]. The corresponding approach for the Helmholtz free energy function ψ is chosen to

$$\begin{aligned}
\rho_0\,\psi_{\mathrm{eq}}^{\mathrm{vol}}(J,\theta) &= \frac{1}{2}\,K\left[(J-1)^2 + (\ln J)^2\right] - K\,\alpha\,(J-1)\,(\theta-\theta_0) - \rho_0\,c(\theta) \\
\rho_0\,\psi_{\mathrm{eq}}^{\mathrm{iso}}(\hat{\mathbf{C}}) &= c_{10}\left(\mathrm{I}_{\hat{\mathbf{C}}} - 3\right) \\
\rho_0\,\psi_{\mathrm{neq}}(\hat{\mathbf{C}}_{\mathrm{e}}) &= c_{10}^{e}\left(\mathrm{I}_{\hat{\mathbf{C}}_{\mathrm{e}}} - 3\right).
\end{aligned} \tag{36}$$

Equation (36)$_1$ includes a volumetric, mechanical term with the compression modulus K based on the work of [46], a thermal–mechanical coupling term with the coefficient of thermal expansion α and a function $c(\theta)$, which can be determined from calorimetric experiments and which is linked to the heat capacity of the material. The two further equations represent the classical approach of a Neo-Hookean material model and describe geometrically nonlinear material behaviour for the equilibrium elasticity and viscoelasticity with the corresponding material parameters c_{10} and c^e_{10}. Taking Eq. (27) into account and evaluating the second law of thermo-mechanics the results read

$$\begin{aligned} p &= -K\left[(J-1)+\frac{\ln J}{J}\right]+K\,\alpha\,(\theta-\theta_0)\,,\\ s &= \frac{1}{\rho_0}\left(K\,\alpha\,(J-1)+\rho_0\,\frac{\partial c(\theta)}{\partial\theta}\right),\\ \hat{\mathbf{T}} &= 2\,J^{-1}\,c_{10}\,\mathbf{I}+2\,J^{-1}\,c^e_{10}\,\hat{\mathbf{C}}_{\mathrm{i}}^{-1}-\frac{2}{3}J^{-1}\left(c_{10}\,\mathrm{tr}\,\hat{\mathbf{C}}+c^e_{10}\,\mathrm{tr}\,\hat{\mathbf{C}}_{\mathrm{e}}\right)\hat{\mathbf{C}}^{-1}. \end{aligned} \tag{37}$$

The last equation of (37) is now used to compute the second Piola–Kirchhoff stress tensor $\mathbf{S}$ on the reference configuration. Taking into account the transport regulations and relationships

$$\begin{aligned} \mathbf{S} &= J\,\mathbf{F}^{-1}\cdot\left(-p\,\mathbf{I}+\mathbf{T}^{\mathrm{D}}\right)\cdot\mathbf{F}^{-T}=-p\,J\,\mathbf{C}^{-1}+J\,\mathbf{F}^{-1}\cdot\mathbf{T}^{\mathrm{D}}\cdot\mathbf{F}^{-T}\\ \mathbf{T}^{\mathrm{D}} &= \hat{\mathbf{F}}\cdot\hat{\mathbf{T}}\cdot\hat{\mathbf{F}}^{T}\\ \bar{\mathbf{F}}^{-T} &= \bar{\mathbf{F}}^{-1}=J^{-\frac{1}{3}}\,\mathbf{I}\\ \hat{\mathbf{C}}^{-1} &= J^{\frac{2}{3}}\,\mathbf{C}^{-1}\\ \mathrm{tr}\,\hat{\mathbf{C}}_{\mathrm{e}} &= \mathrm{tr}\left(\hat{\mathbf{C}}_{\mathrm{i}}^{-1}\cdot\hat{\mathbf{C}}\right) \end{aligned} \tag{38}$$

the second Piola–Kirchhoff stress tensor can be calculated to the following expression

$$\begin{aligned} \mathbf{S} = -p\,J\,\mathbf{C}^{-1}&+2\,c_{10}\,J^{-\frac{2}{3}}\left(\mathbf{I}-\frac{1}{3}\left(\mathrm{tr}\,\hat{\mathbf{C}}\right)\hat{\mathbf{C}}^{-1}\right)\\ &+2\,c^e_{10}\,J^{-\frac{2}{3}}\left(\hat{\mathbf{C}}_{\mathrm{i}}^{-1}-\frac{1}{3}\,\mathrm{tr}\left(\hat{\mathbf{C}}_{\mathrm{i}}^{-1}\cdot\hat{\mathbf{C}}\right)\hat{\mathbf{C}}^{-1}\right). \end{aligned} \tag{39}$$

Considering the above introduced approach, the evolution equation on the EIIC finally reads as

$$\hat{\mathbf{D}}_{\mathrm{i}}=\overset{\triangle}{\hat{\boldsymbol{\Gamma}}}_{\mathbf{i}}=\frac{2\,c^e_{10}}{\eta(\theta)}\left(\hat{\mathbf{C}}_{\mathrm{e}}-\frac{1}{3}\,\mathrm{tr}\left(\hat{\mathbf{C}}\cdot\hat{\mathbf{C}}_{\mathrm{i}}^{-1}\right)\mathbf{I}\right). \tag{40}$$

Using the definition of the relaxation time $r(\theta)=\frac{\eta(\theta)}{c^e_{10}}$ and the arithmetic operation

$$\dot{\hat{\mathbf{C}}}_{\mathrm{i}}=2\,\hat{\mathbf{F}}_{\mathrm{i}}^{T}\cdot\hat{\mathbf{D}}_{\mathrm{i}}\cdot\hat{\mathbf{F}}_{\mathrm{i}} \tag{41}$$

a representation of the evolution equation is calculated in terms of the material time derivative of the inelastic, isochoric right Cauchy–Green deformation tensor to

$$\dot{\hat{\mathbf{C}}}_{\mathrm{i}}=\frac{4}{r(\theta)}\left(\hat{\mathbf{C}}-\frac{1}{3}\,\mathrm{tr}\left(\hat{\mathbf{C}}\cdot\hat{\mathbf{C}}_{\mathrm{i}}^{-1}\right)\hat{\mathbf{C}}_{\mathrm{i}}\right). \tag{42}$$

This evolution equation is solved in the context of a finite element calculation by the method of [45]. For the inclusion of the temperature-dependent mechanical behaviour, the standard WLF-equation is introduced with the standard parameter $C_1=17.5$, $C_2=52\,\mathrm{K}$, cf. Williams et al. [49]. The glass transition temperature $\theta_{\mathrm{G}}=240\,\mathrm{K}$ was chosen with respect to the investigated elastomer, which was used in Sect. 1 to motivate our modelling approach.

$$\eta(\theta)=\eta_0\,\exp\left(-\frac{C_1(\theta-\theta_{\mathrm{G}})}{C_2+\theta-\theta_{\mathrm{G}}}\right) \tag{43}$$

The thermo-mechanical coupling of the material model takes place via the additional consideration and solution of the heat balance in the form of the first law of thermo-mechanics. Based on the balance of internal energy ϵ and by introducing the Legendre transformation $\epsilon = \psi + \theta\, s$, the heat conduction equation is derived to

$$\rho_0\, \dot{\psi} + \rho_0\, \dot{\theta}\, s + \rho_0\, \theta\, \dot{s} = \mathbf{S} : \dot{\mathbf{E}} - \operatorname{Div} \mathbf{Q}. \tag{44}$$

After calculating the stress power and use of the temporal derivative of the free energy function ψ, this expression can be reformulated and simplified. The result has the following form

$$\rho_0\, \theta\, \dot{s} + \operatorname{Div} \mathbf{Q} - c^e_{10}\, \hat{\mathbf{C}}_{\mathrm{i}}^{-1} \cdot \hat{\mathbf{C}} \cdot \hat{\mathbf{C}}_{\mathrm{i}}^{-1} : \dot{\hat{\mathbf{C}}}_{\mathrm{i}} = 0. \tag{45}$$

The first term contains the temporal change of the entropy, the second term is the divergence of the heat flow, and the third term provides the dissipative heating of the material. Calculating the time derivative

$$\dot{s} = \frac{1}{\rho_0} \left(K\, \alpha\, \dot{J} + \rho_0\, \frac{\partial^2 c(\theta)}{\partial\, \theta^2}\, \dot{\theta} \right), \tag{46}$$

taking Fourier's law into account and using an approach for $c(\theta)$ so that

$$\frac{\partial^2 c(\theta)}{\partial\, \theta^2} = \frac{A}{\theta} + B, \tag{47}$$

holds, the heat conduction equation reads:

$$K\, \alpha\, \theta\, \dot{J} + \rho_0\, (A + B\, \theta)\, \dot{\theta} - \lambda_\theta \operatorname{Div} \operatorname{Grad} \theta - c^e_{10}\, \hat{\mathbf{C}}_{\mathrm{i}}^{-1} \cdot \hat{\mathbf{C}} \cdot \hat{\mathbf{C}}_{\mathrm{i}}^{-1} : \dot{\hat{\mathbf{C}}}_{\mathrm{i}} = 0. \tag{48}$$

The first term describes the so-called Gough–Joule effect of elastomers, A and B are introduced material parameters which can be determined via calorimetric experiments and λ_θ is the parameter of the heat conductivity. Equation (47) is motivated via experimental investigations on the caloric behaviour on an elastomer done by Dippel [10].

3 Results and discussion

In order to show the capability of the developed model, some simulations are carried out. Therefore, the presented material model is implemented in the open-source FE-code PANDAS [12]. Therefore, the local balance equations of internal energy (45) and of the momentum are transferred to their weak form by multiplying them with a testing function and integrating them over the calculated body's volume.

The numerical values of the model parameters are given in Table 1. The density ρ_0, the linear coefficient of the thermal expansion α, the caloric parameters A and B and the heat conductivity λ_θ were chosen with respect to the experimental observations of Dippel [10]. It is the same material which was used in Sect. 1.2 to motivate the presented theoretical approach. The other model parameters are selected on the basis of many years of experience regarding the viscoelastic behaviour of elastomers. Moreover, they are tuned in that way that the numerical results show the significant effects of dissipative heating.

As a simplification, the elastic parameter c_{10} describing the equilibrium part of the mechanical behaviour is chosen as temperature independent. The influence of the temperature on the mechanical behaviour is considered with the formulation of the viscosity $\eta(\theta)$. This leads to a lower viscosity with higher temperatures. In order to guarantee mechanically incompressible behaviour, the bulk modulus K is considered as approximately three decades larger than the shear modulus.

With the presented set of parameters, the material model can be validated qualitatively by performing FE calculations of some standard experiments. Therefore, a simple plain strain geometry with 30x50 elements is

Table 1 Set of parameters

ρ_0 kg/m^3	K MPa	α 1/K	$A + B\,\theta$ J/kg·K	λ_θ W/m·K	c_{10} MPa	c^e_{10} MPa	η_0 MPa s
1130	1000	$2.155 \cdot 10^{-4}$	$540 + 3.6\,\theta$	0.225	0.686	0.4	$5 \cdot 10^4$

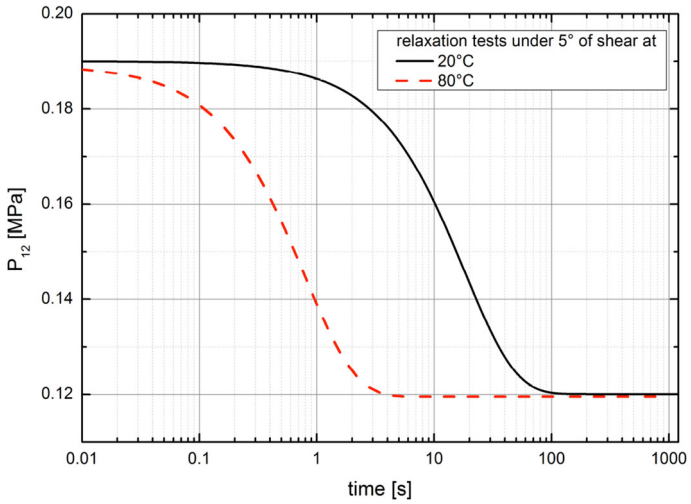

Fig. 4 FE calculations of relaxation tests with a shear angle of 5° and different temperatures of 20 and 80 °C

loaded with different boundary conditions. The ansatz functions for the elements are formulated linearly for the displacement and the temperature.

The first boundary conditions which are applied, are those for a relaxation test under isothermal conditions. Therefore, a constant shear strain $\tan\alpha = \gamma = u/h = 0.000875$ is applied. This corresponds to a shear angle of $\alpha = 5°$. Due to the viscoelastic material behaviour the induced shear stress should decrease over time, after the deformation is applied. The results are presented in Fig. 4. With increasing temperature, the stress relaxation runs faster.

As it is the main focus of this contribution, in further investigations the self-heating under cyclic deformations is calculated. As it can be seen experimentally (see Sect. 1.2), this self-heating is dependent on both the frequency and the amplitude of the deformation. Equation (45) contains both of these influences. The reason for the self-heating is the non-equilibrium stress, the inelastic deformation and its rate. Under a constant frequency, a higher shear amplitude induces higher inelastic deformation rates, as well as it is the case for higher frequencies under constant amplitudes.

The first case is simulated in Fig. 6. There, the development of the temperature over the loading cycles is plotted for sinusoidal shear loading conditions $u(t) = u_0 \sin(2\pi f t)$ with a frequency of $f = 2\,\mathrm{Hz}$ and amplitudes of $u_0 = \gamma h = h \tan\alpha$. The associated shear angles α are 20°, 30° and 40°, and the specimen height is assumed to be $h = 0.01\mathrm{m}$. In each simulation, the boundary conditions on the left- and right-hand sides of the specimen are adiabatic. The boundary conditions on the upper and lower side are modelled as isothermal. This temperature also correspondents to the starting temperature of the specimen. Thus, the heat flux occurs in one direction and the temperature profile of the investigated specimen is inhomogeneous, cf. Fig. 5. With respect to the data in Fig. 6, the middle point of the simulated elastomer specimen is recorded. As it is predicted by the model, the higher the amplitude, the higher the amount of self-heating. It can be seen that the temperature development over the loading cycles is nonlinear. The reason is the heat flux over the upper and lower boundaries of the specimen. After a certain amount of cycles, the interaction between self-heating and heat transfer to the environment becomes a stationary process.

The next simulations concern the frequency dependence of the elastomer with regard to the self-heating, cf. Fig. 7. Using a constant shear angle of 40° and three different frequencies of 2, 4 and 20 Hz, it can be shown that higher frequencies have a comparable influence on the temperature as higher amplitudes do.

4 Conclusion and outlook

Based on experimental observations, it has been shown that the temperature plays an important role in elastomers' properties. As relaxation tests have proven, the mechanical properties are significantly influenced by the material's temperature. With cyclic testings under harmonic strains, the self-heating of a NR-mixture has been investigated. By IR-measurements, it can be seen that dynamic deformations lead to a rise of temperature

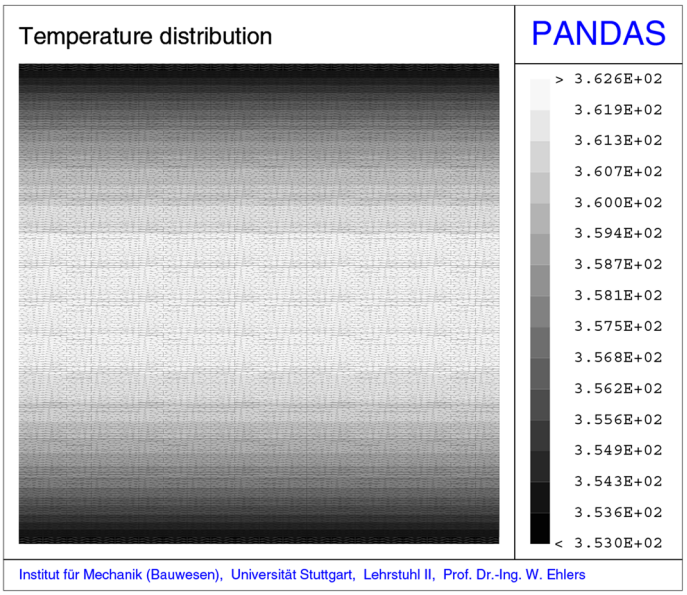

Fig. 5 FE calculation of the inhomogeneous temperature distribution in cyclic shear tests

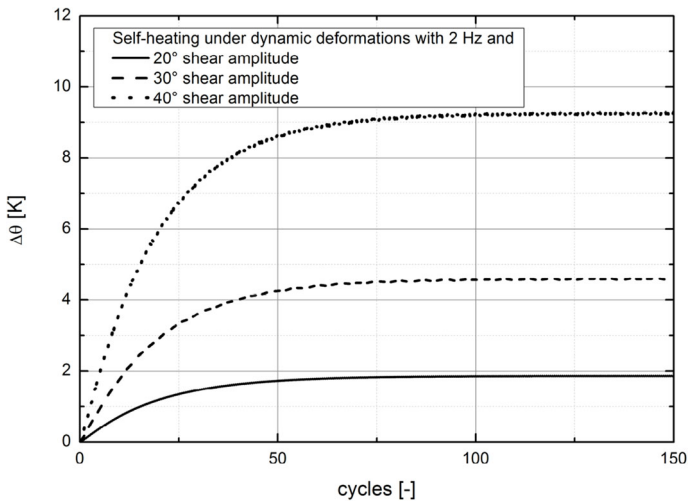

Fig. 6 FE calculations of dynamic shear tests under a constant frequency of 2 Hz and amplitudes of 20°, 30° and 40°

which is not negligible. The measured self-heating is dependent on the applied frequency and deformation amplitude.

Based on these observations, a phenomenological material model is motivated from a macroscopical point of view. It is formulated with respect to large deformations, as it is common for elastomers. The characteristic viscoelastic behaviour is included as well as both the temperature-dependent mechanical properties and the self-heating.

The model was used to carry out exemplaric FE calculations, which show the capability of the model to represent all of the measured effects in a qualitative manner. In a further step, the model's parameters have to be identified using adequate experimental results, such as stepwise tension tests and relaxation tests to identify both the equilibrium part of the mechanical behaviour and the time-dependent influences. As it is the main focus of the presented model, the parameters have to fit the self-heating behaviour measured under dynamic loads. Therefore, it is necessary to formulate the thermal boundary conditions in dependence of the heat transfer with the surrounding media.

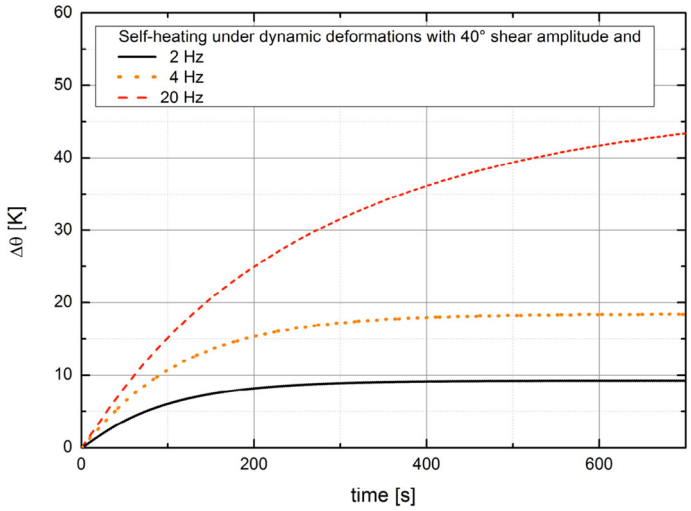

Fig. 7 FE calculations of dynamic shear tests with a constant shear angle of 40° and frequencies of 2, 4 and 20 Hz

Another point on which is to work is the calculation time needed for dynamic simulations. In the current state of a prototypical implementation, calculations of dynamic processes are highly time-consuming. Each result presented in the Figs. 6 and 7 takes about 3 h of calculation, which is unacceptable for commercial use.

References

1. Alts, T.: On the energy-elasticity of rubber-like materials. Prog. Coll. Pol. Sci. S **66**, 367–375 (1979)
2. Amin, A., Lion, A., Sekita, S., Okui, Y.: Nonlinear dependence of viscosity in modeling the rate-dependent response of natural and high damping rubbers in compression and shear: experimental identification and numerical verification. Int. J. Plast. **22**, 1610–1657 (2006)
3. Anand, L., Ames, N.M., Srivastava, V., Chester, S.A.: A thermo-mechanically coupled theory for large deformations of amorphous polymers. Part I: formulation. Int. J. Plast. **25**, 1474–1494 (2009)
4. Arruda, E.M., Boyce, M.C.: A three-dimensional constitutive model for the large stretch behavior of rubber elastic materials. J. Mech. Phys. Solids **41**, 389–412 (1993)
5. Chadwick, P.: Thermo-mechanics of rubberlike materials. Philos. Trans. R. Soc. Lond. A **276**, 371–403 (1974)
6. Cho, H., Bartyczak, S., Mock, W., Boyce, M.C.: Dissipation and resilience of elastomeric segmented copolymers under extreme strain rates. Polymer **54**, 5952–5964 (2013)
7. Coleman, B.D., Gurtin, M.E.: Thermodynamics with internal variables. J. Chem. Phys. **47**, 597–613 (1967)
8. Coleman, B.D., Noll, W.: The thermodynamics of elastic materials with heat conduction and viscosity. Arch. Rat. Mech. Anal. **13**, 167–178 (1963)
9. Dargazany, R., Khîem, V.N., Itskov, M.: A generalized network decomposition model for the quasi-static inelastic behaviour of filled elastomers. Int. J. Plast. **63**, 94–109 (2014)
10. Dippel, B.: Experimentelle Charakterisierung, Modellierung und FE-Berechnung thermomechanischer Kopplungen am Beispiel eines rußgefüllten Naturkautschuks. Ph.D. thesis. Universität der Bundeswehr München (2015)
11. Dippel, B., Johlitz, M., Lion, A.: Thermo-mechanical couplings in elastomers—experiments and modelling. Z. Angew. Math. Mech. doi:10.1002/zamm.201400110 (2014)
12. Ehlers, W., Ellsiepen, P.: PANDAS: Ein FE-System zur Simulation von Sonderproblemen der Bodenmechanik. In: Wriggers, P., Meißner, U., Stein, E., Wunderlich, W. (eds.) Finite Elemente in der Baupraxis: Modellierung, Berechnung und Konstruktion, Beiträge zur Tagung FEM '98 an der TU Darmstadt am 5. und 6. März 1998, pp. 431–400. Ernst & Sohn, Berlin (1998)
13. Göktepe, S., Miehe, C.: A micro-macro approach to rubber-like materials. Part III: The micro-sphere model of anisotropic Mullins-type damage. J. Mech. Phys. Solids **53**, 2259–2283 (2005)
14. Haupt, P.: Continuum Mechanics and Theory of Materials. Springer, Berlin (2000)
15. Haupt, P., Lion, A.: On finite linear viscoelasticity of incompressible isotropic materials. Acta Mech. **159**, 87–124 (2002)
16. Haupt, P., Tsakmakis, C.: On the application of dual variables in continuum mechanics. Continuum Mech. Thermodyn. **1**, 165–196 (1989)
17. Höfer, P., Lion, A.: Modelling of frequency- and amplitude-dependent material properties of filler-reinforced rubber. J. Mech. Phys. Solids **57**, 500–520 (2009)
18. Horstemeyer, M.F., Bammann, D.J.: Historical review of internal state variable theory for inelasticity. Int. J. Plast. **26**, 1310–1334 (2010)
19. Huber, N., Tsakmakis, C.: Finite deformation viscoelasticity laws. Mech. Mater. **32**, 1–18 (2000)
20. Johlitz, M., Scharding, D., Diebels, S., Retka, J., Lion, A.: Modelling of the thermo-viscoelastic material behaviour of polyurethane close to the glass transition temperature. Z. Angew. Math. Mech. **90**, 387–398 (2009)

21. Kaliske, M., Heinrich, G.: An extended tube-model for rubber elasticity: statistical-mechanical theory and finite element implementation. Rubber Chem. Technol. **72**, 602–632 (1999)
22. Keck, J.: Zur Beschreibung finiter Deformation von Polymeren, Experimente, Modellbildung, Parameteridentifikation und Finite-Elemente-Formulierung. Dissertation, Bericht-Nr. I-5 des Instituts für Mechanik (Bauwesen), Lehrstuhl I, Universität Stuttgart (1998)
23. Khan, A.S., Lopez-Pamies, O., Kazmi, R.: Thermo-mechanical large deformation response and constitutive modeling of viscoelastic polymers over a wide range of strain rates and temperatures. Int. J. Plast. **22**, 581–601 (2006)
24. Krempl, E., Khan, F.: Rate (time)-dependent deformation behaviour: an overview of some properties of metals and solid polymers. Int. J. Plast. **19**, 1069–1095 (2003)
25. Lin, R.C., Brocks, W.: On a finite strain viscoplastic theory based on a new internal dissipation inequality. Int. J. Plast. **20**, 1281–1311 (2004)
26. Lin, R.C., Brocks, W., Betten, J.: On internal dissipation inequalities and finite strain inelastic constitutive laws: theoretical and numerical comparisons. Int. J. Plast. **22**, 1825–1857 (2006)
27. Lion, A.: A constitutive model for carbon black filled rubber, experimental results and mathematical representation. Continuum Mech. Thermodyn. **8**, 153–169 (1996)
28. Lion, A.: On the large deformation behaviour of reinforced rubber at different temperatures. J. Mech. Phys. Solids **45**, 1805–1834 (1997)
29. Lion, A.: A physically based method to represent the thermo-mechanical behaviour of elastomers. Acta Mech. **123**, 1–25 (1997)
30. Lion, A.: Thermomechanik von Elastomeren. Berichte des Instituts für Mechanik der Universität Kassel (Bericht 1/2000) (2000)
31. Lion, A., Dippel, B., Liebl, C.: Thermomechanical material modelling based on a hybrid free energy density depending on pressure, isochoric deformation and temperature. Int. J. Solids Struct. **51**, 729–739 (2014)
32. Lion, A., Kardelky, C.: The payne effect in finite viscoelasticity: constitutive modelling based on fractional derivatives and intrinsic time scales. Int. J. Plast. **20**, 1313–1345 (2004)
33. Lubliner, J.: A model of rubber viscoelasticity. Mech. Res. Commun. **12**, 93–99 (1985)
34. Miehe, C., Göktepe, S.: A micro-macro approach to rubber-like materials. Part II: the micro-sphere model of finite rubber viscoelasticity. J. Mech. Phys. Solids **53**, 2231–2258 (2005)
35. Miehe, C., Göktepe, S., Lulei, F.: A micro-macro approach to rubber-like materials. Part I: the non-affine micro-sphere model of rubber elasticity. J. Mech. Phys. Solids **52**, 2617–2660 (2004)
36. Miehe, C., Keck, J.: Superimposed finite elastic–viscoelastic–plastoelastic stress response with damage in filled rubbery polymers. Experiments, modelling and algorithmic implementation. J. Mech. Phys. Solids **48**, 323–365 (2000)
37. Mooney, M.: A theory of large elastic deformation. J. Appl. Phys. **11**, 582–592 (1940)
38. Österlöf, R., Wentzel, H., Kari, L., Diercks, N., Wollscheid, D.: Constitutive modelling of the amplitude and frequency dependency of filled elastomers utilizing a modified Boundary Surface Model. Int.J. Solids. Struct. **51**(19–20), 3431–3438 (2014)
39. Reese, S.: A micromechanically motivated material model for the thermo-viscoelastic material behaviour of rubber-like polymers. Int. J. Plast. **19**, 909–940 (2003)
40. Reese, S., Govindjee, S.: Theoretical and numerical aspects in the thermo-viscoelastic material behaviour of rubber-like polymers. Mech. Time Depend. Mater. **1**, 357–396 (1998)
41. Reese, S., Govindjee, S.: A theory of finite viscoelasticity and numerical aspects. Int. J. Solids Struct. **35**, 3455–3482 (1998)
42. Rendek, M., Lion, A.: Amplitude dependence of filler-reinforced rubber: experiments, constitutive modelling and fem – implementation. Int. J. Solids Struct. **47**, 2918–2936 (2010)
43. Rodas, C.O., Zaïri, F., Naït-Abdelaziz, M.: A finite strain thermo-viscoelastic constitutive model to describe the self-heating in elastomeric materials during low-cycle fatigue. J. Mech. Phys. Solids **64**, 396–410 (2014)
44. Sedlan, K.: Viskoelastisches Materialverhalten von Elastomerwerkstoffen, Experimentelle Untersuchung und Modellbildung. Dissertation, Berichte des Instituts für Mechanik (2/2001), Universität Gesamthochschule Kassel (2001)
45. Shutov, A., Landgraf, R., Ihlemann, J.: An explicit solution for implicit time stepping in multiplicative finite strain viscoelasticity. Comput. Methods Appl. Mech. Eng. **265**, 213–225 (2013)
46. Simo, J.C., Taylor, R.L.: Penalty function formulations for incompressible nonlinear elastostatics. Comput. Meth. Appl. Mech. Eng. **35**, 107–118 (1982)
47. Treloar, L.: The Physics of Rubber Elasticity, 3rd edn. Clarendon Press Oxford (1975)
48. Vandenbroucke, A., Laurent, H., Hocine, N.A., Rio, G.: A hyperelastic-visco-hysteresis model for an elastomeric behaviour: experimental and numerical investigations. Comput. Mater. Sci. **48**, 495–503 (2010)
49. Williams, M.L., Landel, R.F., Ferry, J.D.: The temperature dependence of relaxation mechanisms in amorphous polymers and other glass-forming liquids. J. Am. Chem. Soc. **77**, 3701–3707 (1955)
50. Wollscheid, D., Lion, A.: Predeformation- and frequency-dependent material behaviour of filler-reinforced rubber: experiments, constitutive modelling and parameter identification. Int. J. Solids Struct. **50**, 1217–1225 (2013)